Hindawi
Journal of Nanomaterials
Volume 2023, Article ID 8235077, 15 pages
https://doi.org/10.1155/2023/8235077

Research Article

Optimization of Filler Content and Size on Mechanical Performance of Graphene/Hemp/Epoxy-Based Hybrid Composites using Taguchi with ANN Technique

L. Natrayan,[1] **A. Bhaskar**,[2] **Pravin P. Patil**,[3] **S. Kaliappan**,[4] **M. Dineshkumar**,[5] **and E. S. Esakkiraj**[6]

[1]*Department of Mechanical Engineering, Saveetha School of Engineering, SIMATS, Chennai 602105, Tamil Nadu, India*
[2]*Department of Mechanical Engineering, SRM Institute of Science and Technology, Ramapuram, Chennai 600089, Tamil Nadu, India*
[3]*Department of Mechanical Engineering, Graphic Era Deemed to be University, Bell Road, Clement Town, Dehradun 248002, Uttarakhand, India*
[4]*Department of Mechanical Engineering, Velammal Institute of Technology, Chennai 601204, Tamil Nadu, India*
[5]*Department of Mechanical Engineering, Kongunadu College of Engineering and Technology, Trichy 621215, Tamil Nadu, India*
[6]*Department of Mechanical Engineering, Dambi Dollo University, Dambi Dollo, Ethiopia*

Correspondence should be addressed to L. Natrayan; natrayan07@gmail.com and E. S. Esakkiraj; essakkiraj@dadu.edu.et

Received 12 August 2022; Revised 9 October 2022; Accepted 25 January 2023; Published 22 February 2023

Academic Editor: S. K. Khadheer Pasha

Copyright © 2023 L. Natrayan et al. This is an open access article distributed under the Creative Commons Attribution License, which permits unrestricted use, distribution, and reproduction in any medium, provided the original work is properly cited.

The usage of nanofillers in composite materials has grown over time due to various benefits, including superior properties, better adhesion, and high stiffness. To accomplish this, 150, 200, 250, and 300 gsm of hemp fiber mat with various thicknesses and weight proportions of graphene powder, including 0%, 3%, 6%, and 9%, as well as 3, 6, 18, and 25 μm-sized particles, were used. High-speed mechanical stirring was used to evenly mix the nanofiller (nanographene) with the epoxy-based nanocomposites at various loadings. We looked at the bending and interlaminar shear strength (ILSS) properties of hybrid nanomaterials. According to the study, adding 300 gsm of hemp epoxy composites filled with 6 wt% nanographene has significantly improved mechanical properties. The development of a forecasting model to determine the mechanical properties using artificial neural networks (ANN). The constructed model has a significant connection with the test findings. A correlation of 0.9724 for the Levenberg–Marquardt training procedure indicates a significant connection between the predicted and experimental artificial neural models. The observational and projected results for bending and ILSS have <3% and 4% errors, corresponding to the ANN prediction and Taguchi L16 matrix. The potential of ANN for forecasting the bending and ILSS of composite materials is expanded by the close relationship between ANN and experimental findings. The following parameters were used in the current study to determine the flexural strength: graphene content (40.79%), graphene size (34.19%), the number of hemp layers (12.57%), and hemp fiber thickness (11.65%). Similar to ILSS, graphene content accounts for 47.82% of the total, with graphene size (27.87%), hemp fiber thickness (11.80%), and the number of hemp layers (also 11.80%) all contributing (11.78%).

1. Introduction

Polymer nanocomposites have long aroused the interest of both business and academia due to their potential and outstanding features, the ease with which they are created, and their relative affordability [1]. Humans also use composite materials for practical and technical applications, notably in the automotive, aerospace, military, and aviation industries [2]. However, once external stresses are applied, these materials are vulnerable to failure mechanisms described as either deformation or breaking, which usually negatively impact their economic viability, durability, or safety [3]. As a result, there has been an increase in interest in researching how deformation and fracture analyses might be used to assess the structural strength of composite materials [4]. When a material's toughness equals the load applied, distortion, or

fracture failures typically occur [5]. Several variables, like stress characteristics (direction, intensity, periodicity, etc.) and composite element qualities [6], can be brought on this. The initial stage of composite breakdown is dislocation failure, defined as a modification in a component's physical size or form that initiates a fracture. A crack occurs whenever the composites are split into two or more parts [7]. A thermoplastic composite material will flex elastically when exposed to a high enough stress distribution for a short period, resulting in a quick and reversible deformation upon unloading, according to basic composites techniques [8]. The deformations without fracture that occur whenever the composite materials are loaded constitute a deformation. Composites that can sustain significant plastic deformation without breaking are considered malleable, while those that can snap easily are said to be brittle [9]. A few studies into the mechanical properties of thermoset or thermoplastic materials were conducted for a while without even a workable and plentiful substance becoming accessible [10].

An indigenous species known as hemp (*Cannabis sativa* L.) is now considered the most environmentally friendly industrial fiber [11]. They resemble the marijuana plant, which might sometimes lead to confusion [12]. Hemp, in contrast to marijuana, has a very low concentration of 9-tetrahydrocannabinol [13]. With a high yield and no fertilizer or insecticides, hemp may be cultivated in temperate areas on a range of well-drained, nonacidic soils [14]. It can reach a height of 2–4 m with a diameter of 5–16 mm [15]. The hemp kernel is considered a low agriculture metabolism crop because of its high hygroscopicity and lignin content. Additional processing can lead to high hemp fibers with an indigestible fiber surface and more customization [16]. Hemp fibers are organized into various architectural morphologies and housed in a matrix of hemicelluloses [17]. Because hemp fiber design has been carefully studied, there is no current literature that provides insightful, practical knowledge. Cannabis fibers are used in construction because they are rougher, longer, tougher, and tougher than other plant materials like cotton. Consequently, over a quarter of the cannabis fibers used in industrial processes are used for composite (airline industry, sporting goods, etc.), architectural and construction materials, geo-textiles, and other purposes. Hemp fibers take on various shapes, densities, morphologies, and traits during their lifetime [18].

The usual loadings of ordinary filaments, dust, graphite, ferrite, and others were used. All the research showed that the filler support marginally enhanced the mechanical properties of the composites by using regular fiber factor layering, which was incredibly hydrophobic and produced an unfavorable interaction with the hydrophobic grid [19]. Thus, several factors, such as the effect of filler hybridization by combining two charges in a comparable matrix, may influence how mechanically composite materials behave [20]. The true significance of this hybridized assistance resides in the fact that it would have morphological connections between the fillers used, regardless of whether they are of two different or comparable types. The hydroxyl radicals on the surfaces of cellulose, lignocellulosic, and regular lignin fibers give the filament its extraordinary polarity and hydrophilicity [21]. Due to its high rigidity, cellulose is the principal ingredient that enhances the mechanical characteristics of composites. As a result, a higher cellulose content is achievable by removing the shapeless fiber segments, which significantly alter the resemblance between the regular fiber and the hydrophilic grid. Many researchers investigated the elimination of crystalline portions of the fiber in experiments. To completely eradicate lignin as an amorphous component, it partially removes nanocrystal particles with a hydroxyl solution (NaOH) and bleaches the fiber. Another efficient chemical process for enhancing the mechanical properties of composites is the silane coupling agent. In addition to natural fibers, researchers have also employed organic carbon compounds to enhance the mechanical properties of composites [22].

However, the impact of mixing fibers in matrices has peaked in improving mechanical qualities. The qualities are further enhanced by including nanoparticles, strengthening the bond between the matrix and the fiber [23]. As a result, nanoparticle use in polyester is also growing in popularity [24]. The various allotropes of carbon may be divided into groups based on the chemical bond involved in hybridization. Carbon's single layer of atoms organized in a two-dimensional honeycomb crystal lattice makes up the allotrope of carbon known as graphene. The covalent sp2 link between the carbon molecules and one free electron gives graphene its conductance. Physiological, biochemical, and biological researchers are very interested in graphene because it is a revolutionary nanoparticle with amazing physical features, such as biomaterials, high specific surface area ratios, exceptionally high thermal conductivity, and good electrical conductivity [25]. The best-known substance for heat conductivity, graphene, is known to have special electrical characteristics. Graphene has been explored as an option for transistor circuits since experimental findings demonstrate that it has an astonishingly high electron density at ambient temperature. Compared to Si and III–V transistors, graphene has an electron transport of over 200 times greater and four times higher, respectively. Due to this, graphite would be a highly favorable choice for elevated circuits [26].

Taguchi analysis is employed to identify the different evaluation characteristics of the composite. Researchers have already employed the Taguchi approach in producing optimum process input variables for better mechanical performance. However, this work tried to use Taguchi and contemporary optimization approaches to improve the process parameters [27]. The current neural system is a statistical simulation tool for irregular input–output data behavior. Optimization makes it simple to link several quantitative and qualitative criteria together. The share market, medical diagnostics, chemical research, and material science have succeeded in applying artificial neural networks (ANNs), a potent mathematical tool [28]. The parallel-operating neurons that make up neural networks are modeled after the biological nervous system. The linear equation between components, which would be frequently exponential, has a significant impact on the accuracy of the predictions, and this ANN may be trained to perform a specific function by changing the weights. As in nature, the friction system has a highly complicated condition, making it nearly impossible to build an exact link between target response and mechanical achievements [29]. The primary feature of this

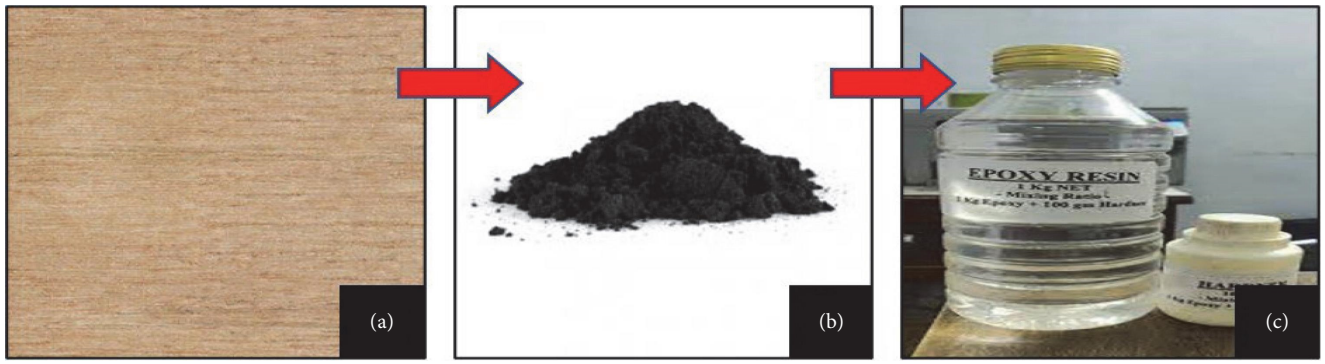

Figure 1: Photographic images of reinforcement and fillers.

approach would be that the neural model is immediately generated from data without any prior assumptions since ANN works like a "black box." The relationship between mechanical characteristics and distinctive feature variables, such as materials, fiber constraints, and mechanical characteristics, would have been formed once a well-executed network was established [30]. This relationship is crucial for designing materials to gratify diverse needs. Extensive research must be done before building a well-functioning neural network, including work on the training method, network topology, volume of training examples, and other factors [31]. Additionally, using ANN to calculate new results might greatly cut the time spent repeating experiments. It is the rationale behind the introduction of the ANN in this area of materials engineering [32].

Fabricating and improving the mechanical characteristics of woven hemp/nanographene/epoxy-based hybrid composites is the main goal of the current research activity. The hybrid composites were created using the L16 Taguchi orthogonal array and the hand lay-up approach. Following manufacture, mechanical tests, such as bending and interlaminar shear strength (ILSS), were conducted. Finally, Taguchi and contemporary ANN were used to optimize the test findings.

2. Experimental Works

2.1. Materials. GVR Fiber Industry delivered the woven hemp fiber mat in Madurai, Tamil Nadu, India. The coir fiber mates were gently laved with clean water and sun-dried for 2 days to eliminate the moisture. After that, the hemp fiber was soaked in a NaOH solution for 4 hr. The fiber was then washed in clean water and put into the weave at a temperature of 75°C. Epoxy and graphene were employed as the matrix in this study. In Chennai, Tamil Nadu, India, Naga Chemicals Industries supplied the graphene fillers and the Matrix. The photographic pictures of reinforcements and fillers are shown in Figure 1(a) exposes the woven hemp fiber mat; (b) shows the graphene filler; and (c) shows the epoxy resign. Table 1 demonstrates the mechanical properties of reinforcement and matrix.

2.2. Nanocomposite Fabrication. Several methods have been used to create thermoplastic nanomaterials. However, a small exception may be made in the case of reinforcement dispersion in the polymer that was effectively carried out in a lab before production using the ultrasonic radiation technique when the composites comprise particles and short fiber reinforcement. Creating carbone natural firebase hybrid nanocomposite samples involves a few fundamental steps. The polymer compositions initially require mixing resin in the right amounts with other chemicals like agents, accelerators, reactive diluents, colors, etc., to get the desired function. A releasing hydrogel agent is applied to the surface of a mold to keep the polymer from adhering to it. A thin plastic sheet is then placed over the top and bottom of the mold plates to produce a level surface for the product. Using a brush, the glue and reinforcements are applied uniformly to the surface of the mold. More mats are placed over the preceding polymeric coating to eliminate trapped air pockets and different polymers. The mold is then sealed, and the steaming environment's pressure is released. After drying at room temperature, the mold is opened, and the nanocomposite is removed from the surface. The hybrid composite combinations are listed in Table 2.

Table 1: Mechanical properties of hemp and epoxy matrix.

Sr. no.	Properties	Hemp fiber	Epoxy resin
1	Cellulose (%)	68.3–69.31	–
2	Hemi cellulose (%)	11–11.64	–
3	Lignin (%)	3.3	–
4	Density (g/cm^3)	1.25	1.16
5	Tensile strength (MPa)	690–930	8–19
6	Young's modulus (GPa)	69–76	0.58
7	Elongation (%)	2.6–3.3	1.6

2.3. Testing. The fabricated composite specimens were cut to ASTM D-790 (width 10 mm, length 125 mm, and thickness 3 mm) for flexural testing and ASTM standard D-2344 was used to measure the ILSS properties of the sample. Under three-point bending, a 45 mm long bar with a minimum thickness (width equals thickness) and square cross segments were loaded.

2.4. Taguchi Approach. Because it requires many investigations, the normal investigative strategy is still too intricate and unrealistic. The Taguchi technique employs fewer experiments.

Table 2: Parameters and their constraints.

Sr. no.	Constrains	Symbols	Stages			
			S1	S2	S3	S4
1	Nanographene (wt%)	A	0	3	6	9
2	Nanographene size (μm)	B	3	6	18	25
3	Hemp fiber thickness (gsm)	C	150	200	250	300
4	Hemp layers (no)	D	1	2	3	4

Table 3: Experimental design and their outcomes.

Run	A	B	C	D	Flexural	ILSS	S/N of flexural	S/N of ILSS
1	0	3	150	1	54.69	35.04	34.758	30.891
2	0	6	200	2	57.63	36.71	35.213	31.296
3	0	18	250	3	61.47	40.82	35.773	32.217
4	0	25	300	4	61.02	40.37	35.709	32.121
5	3	3	200	3	61.75	42.1	35.813	32.486
6	3	6	150	4	57	37.35	35.117	31.446
7	3	18	300	1	64.68	46.04	36.215	33.263
8	3	25	250	2	67.02	47.37	36.524	33.510
9	6	3	250	4	61.14	41.49	35.727	32.359
10	6	6	300	3	66.25	46.6	36.424	33.368
11	6	18	150	2	62.46	42.81	35.912	32.631
12	6	25	200	1	69.14	50.51	36.795	34.068
13	9	3	300	2	64.67	45.02	36.214	33.068
14	9	6	250	1	63.25	44.52	36.021	32.971
15	9	18	200	4	63.09	43.44	35.999	32.758
16	9	25	150	3	68.1	47.45	36.663	33.525

ILSS, interlaminar shear strength.

By using the signal-to-noise (S/N) ratio and analysis of variance (ANOVA), process variables' impacts on mechanical attributes are demonstrated. The Taguchi method of experimental process is a useful way to scientifically explain, examine, and optimize a range of process components to reach the desired result. By translating the investigation's findings into an S/N percentage, this approach allows for the identification of the main constraints. The S/N ratio attributes were classified into three groups based on the strong case for enhancing the main feature: (1) higher was good, (2) nominally better, and (3) lowest was best. The performance characteristic is greater than the S/N ratio regardless of the performance characteristic specified. Therefore, the ideal level for the variable is the one with the largest S/N ratio [6, 7]. Using the greater principle, the composites' bending and ILSSs were assessed throughout the testing procedure. S/N ratios of key attributes are explicitly expressed as follows since bigger is better:

$$\text{S/N ratio} = -10\log_{10}\frac{1}{e}\sum_{s=i}^{e}\frac{1}{X_{\text{st}}^2}. \quad (1)$$

3. Result and Discussion

3.1. Results Based on S/N Ratio. Based on the output circumstances, the S/N ratio of the Taguchi technique was employed to enhance the process parameters of the chosen variables. In the current study, L16 orthogonal arrays were used to create and analyze nanocomposites. The greater the functions, the better the mechanical outcomes in the current study, such as bending and ILSS, were assessed. The present study's findings are influenced by input factors, including the amount of nanographene, the size of the nanoparticles, and the thickness and number of layers of the hemp fiber mat. Minitab 17 was used to conduct the statistical analysis. The S/N ratio of the mechanical characteristics was computed using the maxim "the Larger the Better." The analysis's highest S/N ratio was the study's finest finding [6, 7, 13]. The L16 orthogonal array and S/N ratio of the mechanical results are shown in Table 3. ANOVA and the S/N ratio were used to calculate each variable's impact.

Figures 2(a) and 2(b) depict the impact curve on the S/N ratio for material characteristics. All mechanical properties performed well at the optimal circumstances of 6 wt% graphenes with 25 μm size and 300 gsm of hemp fiber mat with three layers. The bigger and better S/N response displayed the largest mechanical qualities. The controlling variable's impacts on the bending and ILSS characteristics with the S/N ratio response are shown in Tables 4 and 5.

3.2. Analysis of Variance. An ANOVA was carried out to determine the significance of interrupted processing elements.

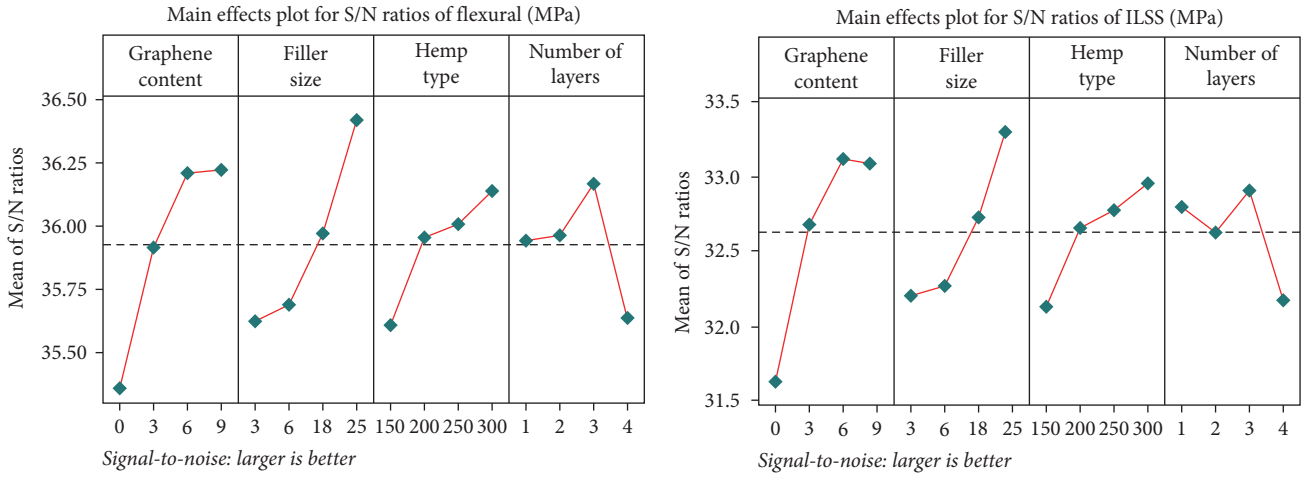

Figure 2: S/N ratio larger the better plot for (a) flexural; (b) interlaminar shear strength properties of nanocomposites.

Table 4: S/N ratio of bending characteristics of nanocomposite.

Levels	Graphene nanopowder (wt%)	Graphene nanopowder size (μm)	Hemp fiber mat thickness (gsm)	Number of layers (no)
1	35.36	35.63	35.61	35.95
2	35.92	35.69	35.95	35.97
3	36.21	35.97	36.01	36.17
4	36.22	36.42	36.14	35.64
Delta	0.86	0.79	0.53	0.53
Rank	1	2	4	3

Table 5: S/N ratio of interlaminar shear strength of nanocomposite.

Levels	Graphene nanopowder (wt%)	Graphene nanopowder size (μm)	Hemp fiber mat thickness (gsm)	Number of layers (no)
1	31.63	32.20	32.12	32.80
2	32.68	32.27	32.65	32.63
3	33.11	32.72	32.76	32.90
4	33.08	33.31	32.95	32.17
Delta	1.47	1.10	0.83	0.73
Rank	1	2	3	4

Figure 3 displays the participation percentage for each component. Tables 6 and 7, columns F display the contribution percentage for each processing parameter. The bending and ILSS properties are assumed to be influenced by the process variable known as the *F*-test. The fraction of the trial's real differences calculated after accounting for each significant effect is known as the contributory percentage [33].

Figure 3(a) shows the percentage impact of processing parameters on mechanical characteristics Figure 3(b). Table 5's *F*-value and contribution % are control factors in achieving the greatest flexibility. According to the previous data, hemp fiber mat thickness is 11.65%, while the wt% of graphene filler is 40.79%, followed by graphene filler size, which contributes 34.14%. Therefore, it is clear that the weight ratio of graphene to filler is the key to achieving excellent mechanical performance. As per Table 6, hemp fiber thickness and the number of layers came in third and fourth place, correspondingly, with 11.80% and 11.78% of the graphene filler weight ratio, which gave 47.82% and 27.87% of the nanographene size, respectively. The results show that the maximum mechanical strength qualities in the current investigation were achieved primarily due to the graphene filler weight ratio and size [34].

3.3. Regression Calculation. The four levels properly considered for this research and four control circumstances were used to build the regression modeling approach. The formulae for bending and ILSS were developed using the conventional regression technique by reducing the total square

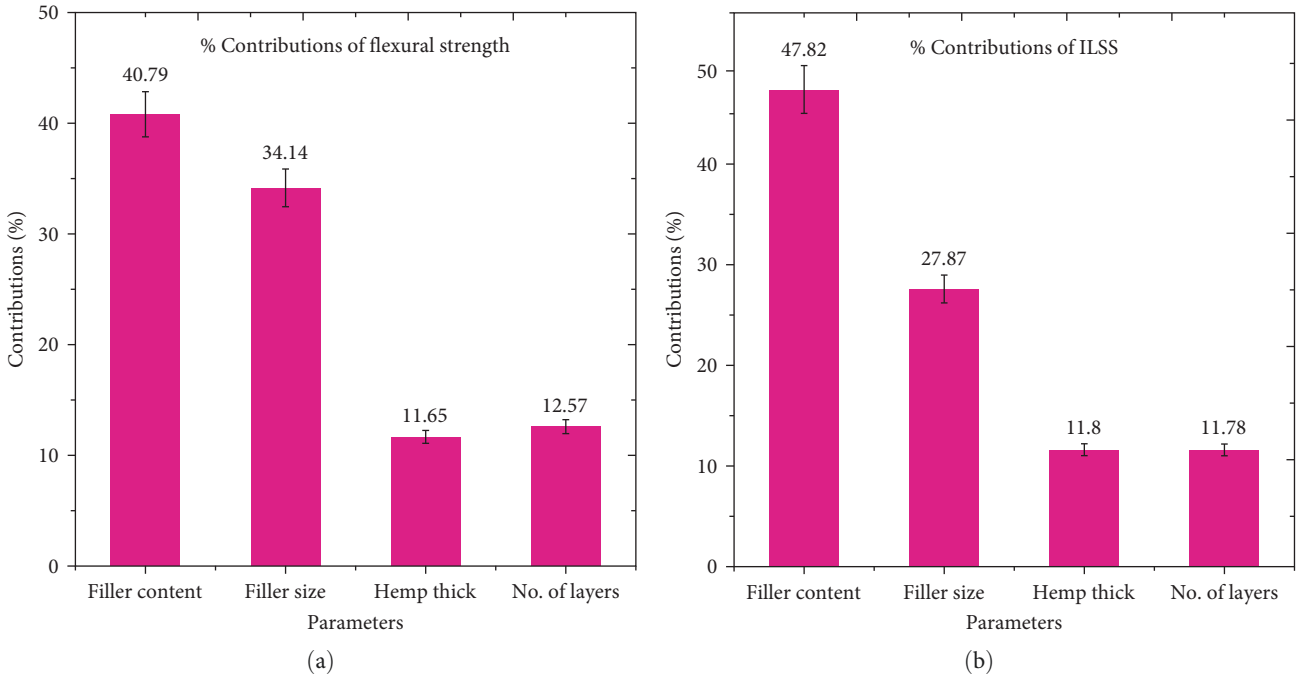

Figure 3: Nanocomposite parameter contributions: (a) bending; (b) interlaminar shear strength.

Table 6: ANOVA for bending behavior.

Source	DF	Seq SS	Contribution	Adj SS	Adj MS	*F*-Value	*P*-Value
Filler content	3	97.982	40.79	90.982	32.660	47.85	0.005
Filler size	3	82.016	34.14	82.016	27.338	40.05	0.006
Hemp type	3	27.988	11.65	27.988	9.329	13.67	0.030
No of layer	3	30.203	12.57	30.203	10.067	14.75	0.027
Error	3	2.048	0.85	2.048	0.682		
Total	15	240.23	100				

Table 7: ANOVA for interlaminar shear strength behavior.

Source	DF	Seq SS	Contribution	Adj SS	Adj MS	*F*-Value	*P*-Value
Filler content	3	130.901	47.82	130.901	43.633	65.48	0.003
Filler Size	3	76.281	27.87	76.281	25.427	38.16	0.007
Hemp type	3	32.292	11.80	32.292	10.764	16.15	0.023
No of layer	3	32.248	11.78	32.248	10.749	16.13	0.024
Error	3	1.999	0.73	1.999	0.666		
Total	15	273.72	100				

profits. The multiple linear regression equation that provides positive indications makes the mechanical and physical properties more valuable, while those that show a negative signal make the mechanical features less valuable. The perfect mixture for all mechanical properties was 300 gsm of three-layered hemp fiber mat and 6 wt% nanographene with a 25 m size. Regression analysis is produced using Equations (2) and (3).

$$\begin{aligned}\text{Flexural} = {} & 62.71 - 4.008\,A1 - 0.097\,A2 + 2.037\,A3 + 2.067\,A4 - 2.14 \\ & B1 - 1.677\,B2 + 0.215\,B3 + 3.610\,B4 - 2.148\,C1 + 0.193\,C2 + 0.510 \\ & C3 + 1.445\,C4 + 0.230\,D1 + 0.235\,D2 + 1.682\,D3 - 2.147\,D4.\end{aligned} \tag{2}$$

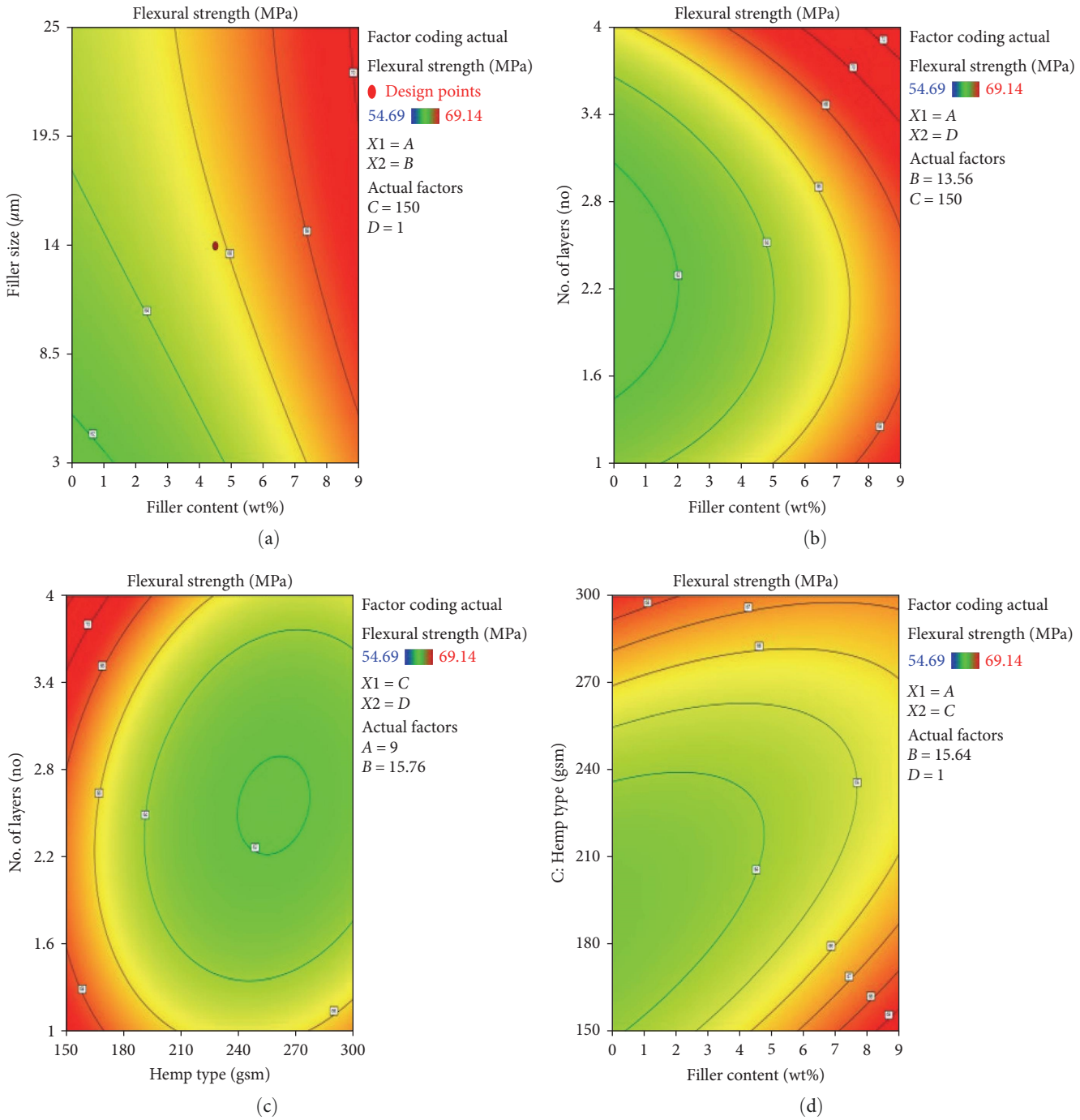

Figure 4: Contour plots of flexural characteristics of graphene-based nanocomposite: (a) filler size vs. fiber content vs. flexural strength; (b) number of layers vs. fiber content vs. flexural strength; (c) hemp type vs. number of layers vs. flexural strength; (d) hemp type vs. fiber content vs. flexural strength.

$$\begin{aligned} \text{ILSS} = {} & 42.978 - 4.743\,A1 + 0.238\,A2 + 2.375\,A3 + 2.130 \\ & A4 - 2.065\,B1 - 1.682\,B2 + 0.300\,B3 + 3.447\,B4 - 2.315\,C1 + 0.213\,C2 + 0.573 \\ & C3 + 1.530\,C4 + 1.050\,D1 + 0.00\,D2 + 1.265\,D3 - 2.315\,D4. \end{aligned} \tag{3}$$

The capacity of organic nanocomposites was increased by up to 6% when a graphene nanofiller was used as a filler. The connection between the reinforcement and the matrix degraded as the wt% of the graphene filler increased [35].

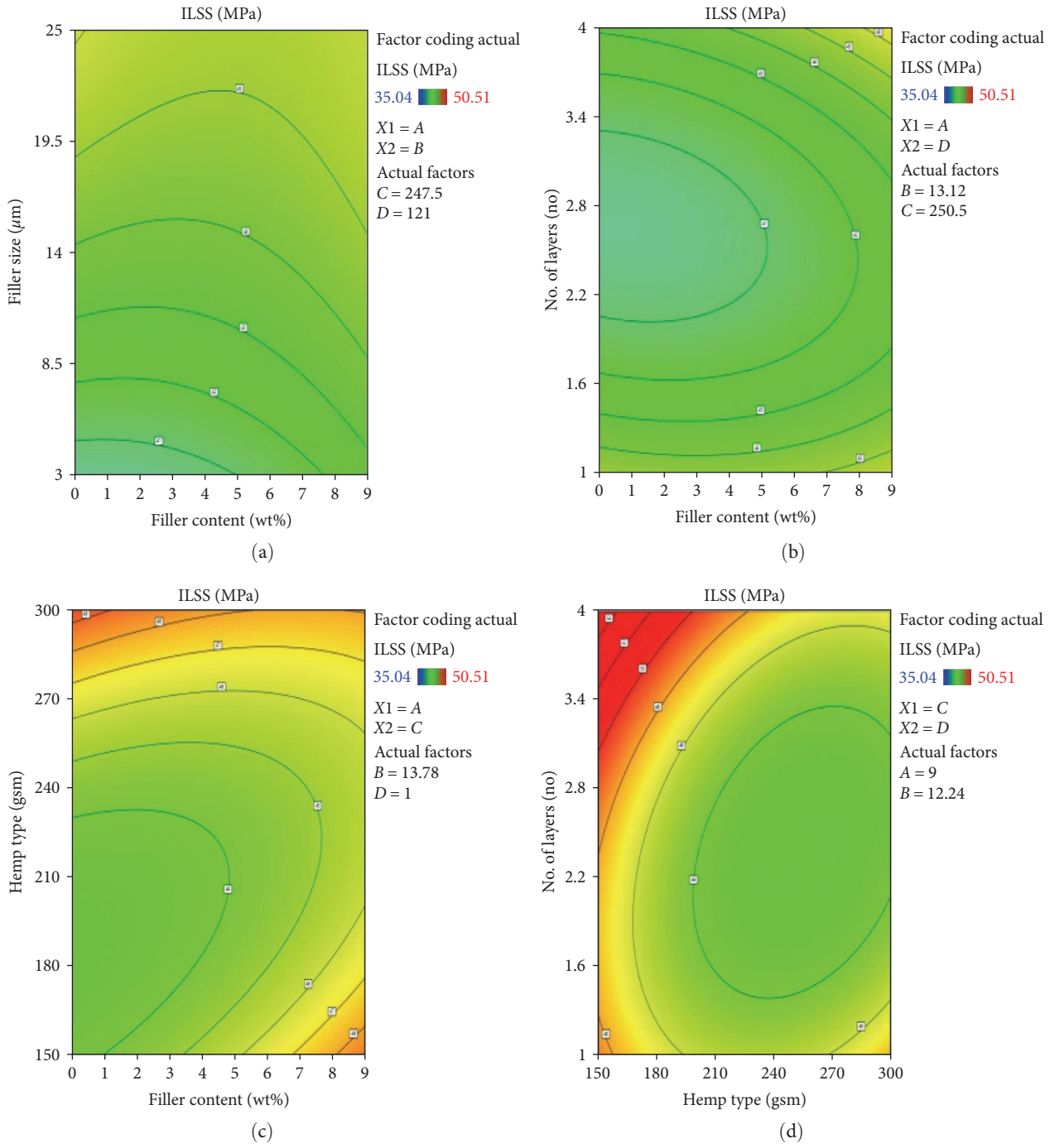

Figure 5: Contour plots of interlaminar shear strength (ILSS) characteristics of graphene-based nanocomposite: (a) filler size vs. fiber content vs. ILSS; (b) number of layers vs. fiber content vs. ILSS; (c) hemp type vs. fiber content vs. ILSS; (d) hemp type vs. number of layers vs. ILSS.

That is the result of improper powder and polymer mixing. Figure 4(a)–4(d) displays the flexural characteristics contour plots about various factors.

The flexural tests reveal that the graphene and hemp fiber-based composite specimens have a substantially greater flexural modulus than epoxy-based composites. This result seems to be explained by the porous structure of graphene and natural fiber filaments. Despite this, the barrier appeared to be increased, and the modest contents (25 μm) seemed swiftly spread along the adhesion strength. Contrary to nanoparticles that exhibit outstanding mechanical strength with a large filler size (25 μm), increasing fiber content has a propensity to agglomerate, which further inhibits better results in mechanical features. The structure was less sturdy and soon deformed with the addition of nanoparticle fillers due to defects and voids at the μm level [36]. The thickness of the hemp fiber is advantageous on all fronts. It demonstrates that a stronger hemp weave will boost the strength of a nanocomposite so that the consequences of vacancies are lessened by the presence of heavy, high-cellulose components.

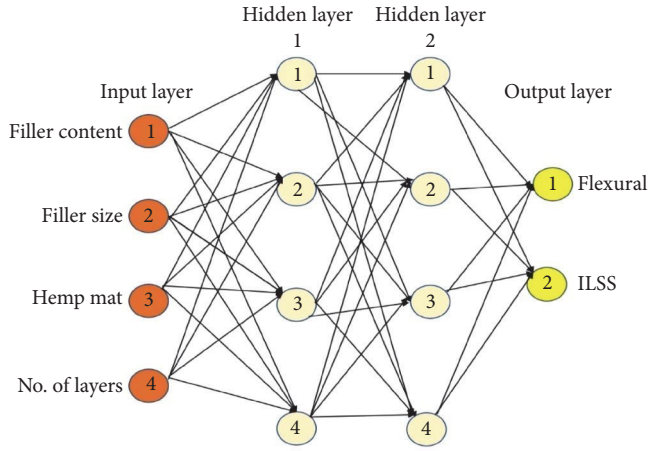

Figure 6: ANN structure of present research work.

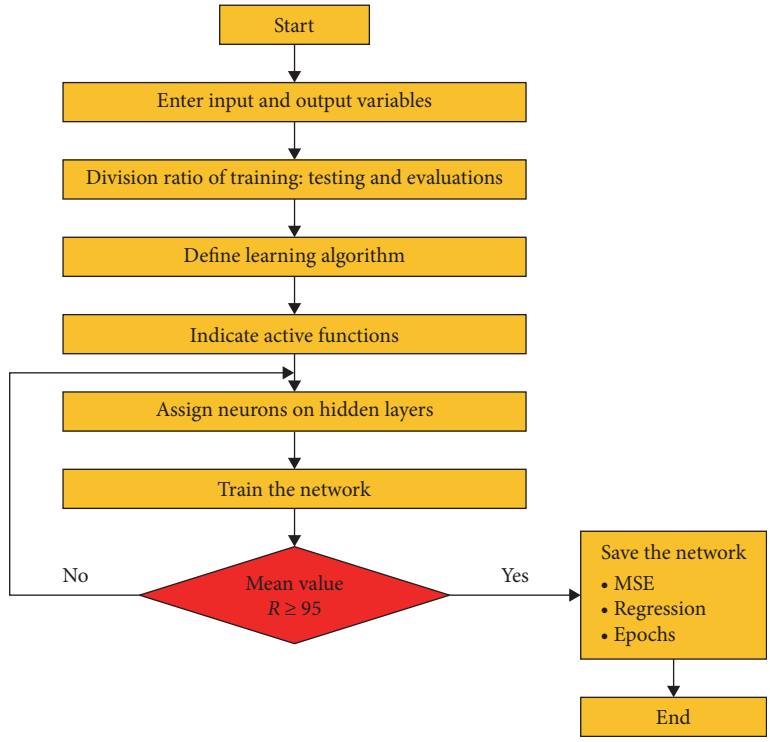

Figure 7: Flowchart of ANN network for the graphene-based nanocomposites.

The amount of energy required to separate the fiber bundles from the matrix increases as the number of layers increases. But up to the third layer, this constructive method was conceivable. The high moisture absorption rate of natural fibers may cause the subsequent loss in mechanical characteristics. The inadequate matrix–fiber contact may also be the cause of the lowest strength. Figure 5(a)–5(d) displays the ILSS characteristics contour plots about various factors. The composite reached its optimum strength when 6 wt% of graphene nanoparticles were added. This finding showed that the addition of nanomaterials to composites improved the qualities of the composite by raising the energy absorption capabilities, surface area, and decreasing the amount of blank land inside the composite material. It shows that adding 6% of graphene filler to epoxy increases its ability to distribute and release tension to the necessary level [37]. Furthermore, this circumstance was probably caused by the uniform distribution of graphene particles inside the matrix, leading to enhanced interactions between the fillers, matrix, and fiber contact area. Consequently, stress transmission was made simpler, and the specimen could withstand greater stress, producing composite samples with enhanced strength.

3.4. Artificial Neural Networks. Study data are acquired using a variety of techniques. ANN connect and evaluate the study data. This model contains three strands: hidden, input, and outcomes. The hidden layer defines optimization, the output unit notifies the controllers, and the input sequence is

Table 8: Comparison of experimental vs. ANN results.

Sr. no.	Experimental results		ANN results		Predicted error	
	Flexural	ILSS	Flexural	ILSS	Flexural	ILSS
1	54.69	35.04	55.11	35.34	−0.768	−0.8505
2	57.63	36.71	58.05	37.01	−0.7288	−0.8118
3	61.47	40.82	61.89	41.12	−0.6833	−0.73
4	61.02	40.37	61.44	40.17	−0.6883	0.49542
5	61.75	42.10	61.23	42.40	0.84211	−0.7078
6	57.00	37.35	57.42	37.14	−0.7368	0.56225
7	64.68	46.04	64.18	46.34	0.77304	−0.6473
8	67.02	47.37	67.44	47.67	−0.6267	−0.6291
9	61.14	41.49	61.56	41.79	−0.6869	−0.7182
10	66.25	46.60	66.20	46.32	0.07547	0.60086
11	62.46	42.81	62.88	43.11	−0.6724	−0.6961
12	69.14	50.51	70.56	51.81	−2.0538	−2.5737
13	64.67	45.02	65.09	45.32	−0.6495	−0.6619
14	63.25	44.52	63.67	44.82	−0.664	−0.6694
15	63.09	43.44	63.51	43.74	−0.6657	−0.686
16	68.10	47.45	67.98	47.11	0.17621	0.71654

ILSS, interlaminar shear strength.

frequently used for information entry. In MATLAB R2015, the ANN approach is utilized to predict mechanical characteristics. The inputs were the graphene filler weight ratio, size of nanofiller, hemp fiber thickness, and the number of hemp layers; the outcomes were bending and ILSS. A feed-forward training algorithm was applied for the estimation of material properties. An ANN was also utilized with the Levenberg–Marquardt (LM) learning method. The buried levels each include four neurotransmitters. The ANN generates three types of inputs: learning (60%), testing (20%), and confirmation (20%). Figure 6 shows the ANN structure of the present research work.

Ten of the 16 measures were chosen, with three for investigation and three for validation. The entire dataset and results were sent to the ANN. It provides the network's independent test [38]. While either one or two neurotransmitters were created in the hidden layer, four neurotransmitters are related to four characteristics generated in the output unit [39]. The input networks' predefined input factors affect four neurotransmitters. After the network had been built, specifically provided data sets were added to the 4-4-4-2 ANN architecture [40]. It may be seen in Figure 6. The model was assessed using correlation analysis and a proportionate confidence interval. Figure 7 depicts the whole flow diagram for the ANN prognostication. The established ANN system uses an equation to determine the predicted average error (Equation (4)).

$$\%\ \text{Of predicted error} = \frac{\text{experimental data} - \text{ANN data}}{\text{experimental data}} \times 100. \tag{4}$$

The training, confirmation, and evaluation groups of metrics are shown in Table 8, together with the prediction error percentage. Figures 8(a) and 8(b) show how well the neural model suggests the future. The reliability for all variables was 0.9724 for bending and 0.9747 for ILSS, and the mean percentage of anticipated error (0.9512) became <3%. It is demonstrated in Figure 9. ANN model error plots for flexural and ILSS are shown in Figures 9(a) and 9(b). Figures 10(a) and 10(b) illustrate the research findings and the relationship between network adaptability. Experiment evaluation was carried out once the measurement items were inside the ideal ranges [41]. Figure 9 summarizes the accuracy of the research, prediction, and ANN models. It is used to evaluate the integrity of the experimental data.

The analysis of experimental evidence has shown that the Taguchi and ANN techniques yield reliable results. The ANN technique produced better results than Taguchi's calculated observations, yielding more accurate forecasts with a 95% dependability rate. Integrating the sources of variation that lead to a particular cast composite is made easier by the ANN optimal model. This is perfect for the areas of the vehicle industry that use natural fibers since it reduces costs. Based on empirical, regression, and ANN findings, Table 9 shows the best mechanical property performance.

4. Conclusion

The bending and ILSS behavior of various-sized graphene-based hemp/epoxy hybrid composites are studied in the current research. Taguchi, regression, and ANN models were used to analyze the results of the composites. The outcomes that followed were attained.

(1) According to the Taguchi study, the following processing parameters offer the maximum mechanical strength. 300 gsm hemp fiber mat with three layers, 6% graphene, and a size of 25 μm.

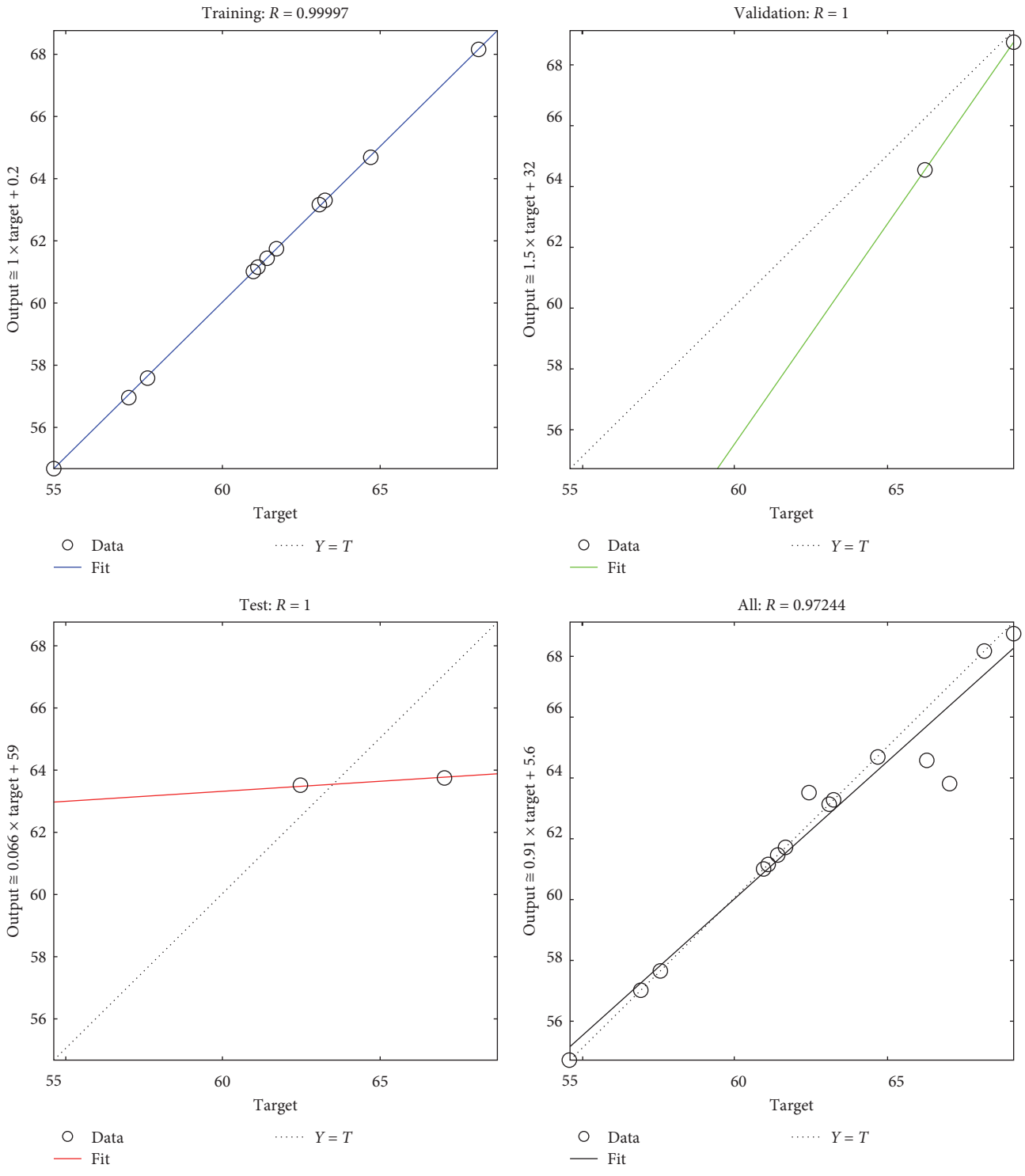

(a)

Figure 8: Continued.

(2) The closeness of the coefficient of correlation, which is closer to 1, shows that the ANN model and the actual outcomes strongly correlate. The absolute percentage of mean inaccuracy is <1%. This proof demonstrates the ANN model's capacity to predict composites' bending and ILSS.

(3) The following parameters were used in the current study to determine the flexural strength: graphene

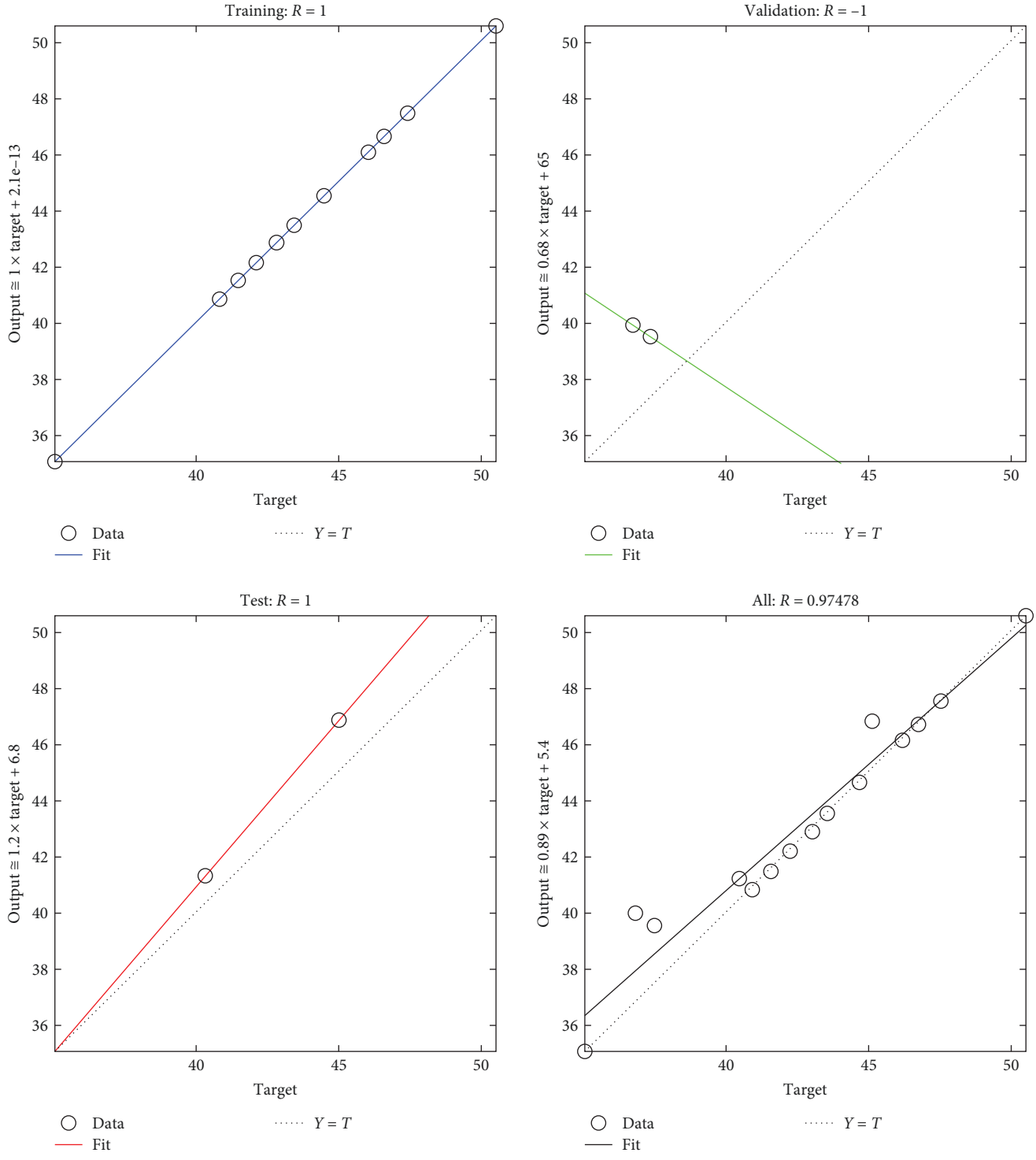

(b)

Figure 8: Performance features of ANN model: (a) flexural behavior; (b) interlaminar shear strength behavior.

content (40.79%), graphene size (34.19%), the number of hemp layers (12.57%), and hemp fiber thickness (11.65%).

(4) Similar to ILSS, graphene content accounts for 47.82% of the total, with graphene size (27.87%), hemp fiber thickness (11.80%), and the number of hemp layers (also 11.80%) all contributing (11.78%).

(5) With the LM algorithm, a network may be created without such data being fascia, and the least mean square errors can be obtained. The ANN model changes depending on the architecture being utilized.

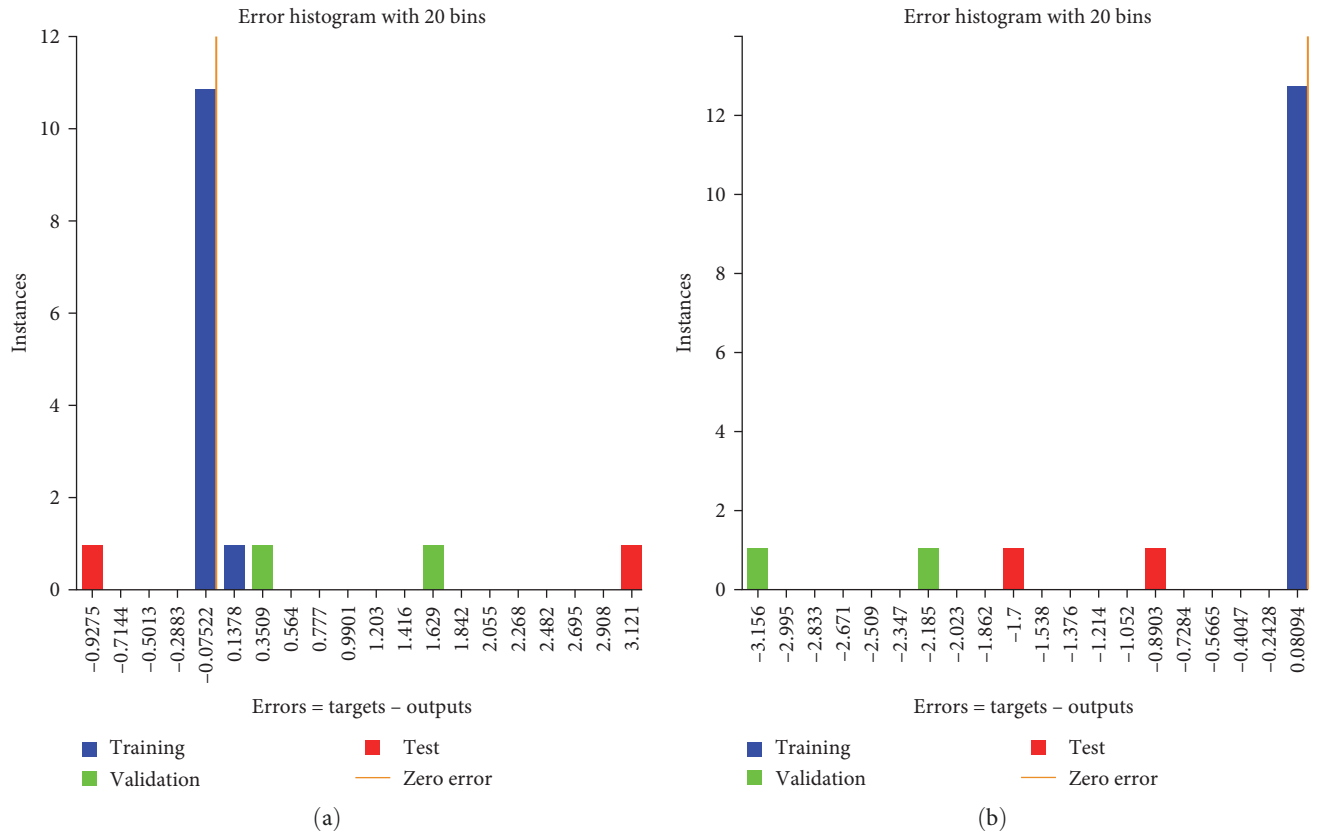

Figure 9: ANN model error plots for (a) flexural; (b) interlaminar shear strength behavior.

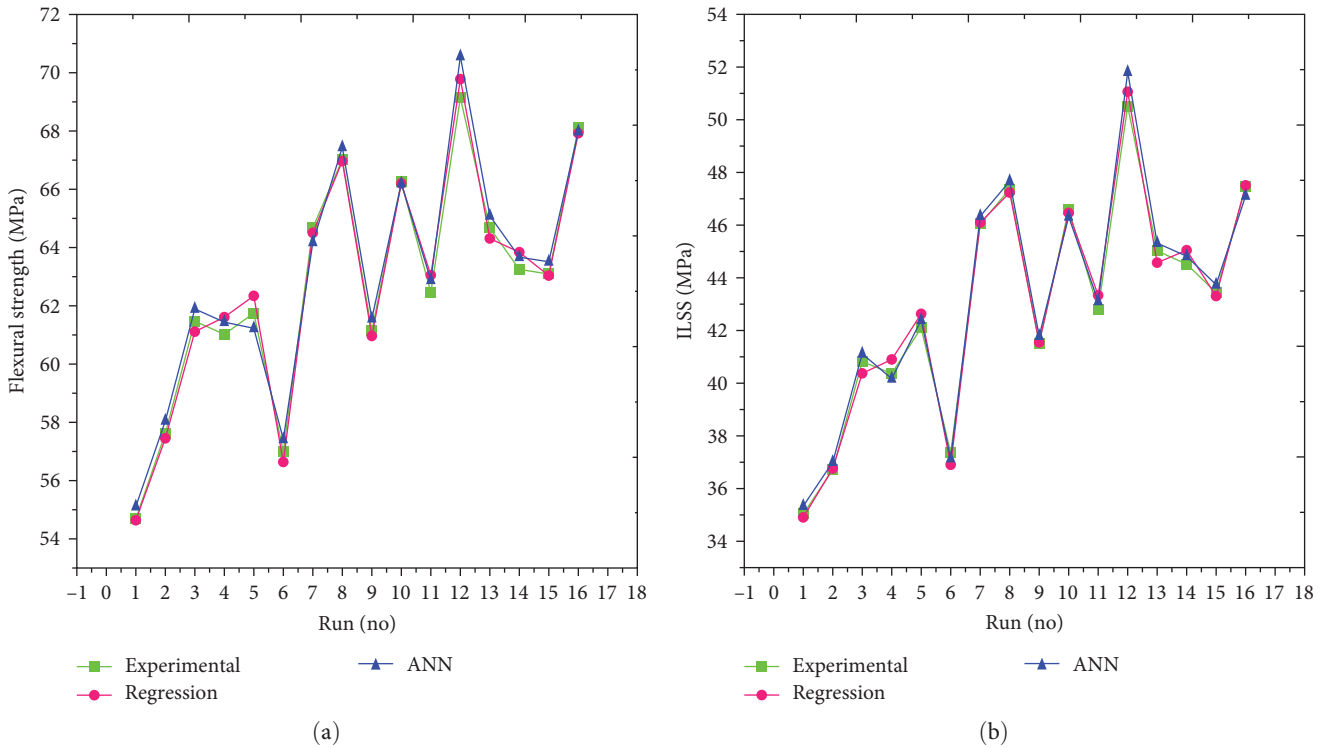

Figure 10: Comparison of experimental/regression/ANN outcomes of graphene-based hybrid composites: (a) flexural strength; (b) interlaminar shear strength behavior.

Table 9: Optimum outcomes of nanocomposites.

Outcomes	Parameter levels	Investigational model	Regression model	ANN model
Flexural (MPa)	*A*3, *B*4, *C*4, *D*2	69.14	69.78	70.56
ILSS (MPa)	*A*3, *B*4, *C*4, *D*2	50.51	51.06	51.81

ILSS, interlaminar shear strength.

Therefore, it is recommended to start developing the model using a variety of neurons. The greatest findings for forecasting mechanical properties in this investigation came from 10 neurons.

Data Availability

The data used to support the findings of this study are included in the article. Should further data or information be required, these are available from the corresponding author upon request.

Conflicts of Interest

The authors declare that they have no conflicts of interest.

References

[1] D. Bonamy and E. Bouchaud, "Failure of heterogeneous materials: a dynamic phase transition?" *Physics Reports*, vol. 498, no. 1, pp. 1–44, 2011.

[2] J. H. Keyak and S. A. Rossi, "Prediction of femoral fracture load using finite element models: an examination of stress-and strain-based failure theories," *Journal of Biomechanics*, vol. 33, no. 2, pp. 209–214, 2000.

[3] F. Berto and P. Lazzarin, "Recent developments in brittle and quasi-brittle failure assessment of engineering materials by means of local approaches," *Materials Science and Engineering: R: Reports*, vol. 75, pp. 1–48, 2014.

[4] S. T. Pinho, P. Robinson, and L. Iannucci, "Developing a four point bend specimen to measure the mode I intralaminar fracture toughness of unidirectional laminated composites," *Composites Science and Technology*, vol. 69, no. 7-8, pp. 1303–1309, 2009.

[5] P. K. Kristensen, C. F. Niordson, and E. Martínez-Pañeda, "Applications of phase field fracture in modelling hydrogen assisted failures," *Theoretical and Applied Fracture Mechanics*, vol. 110, Article ID 102837, 2020.

[6] M. J. DeJong, M. A. N. Hendriks, and J. G. Rots, "Sequentially linear analysis of fracture under non-proportional loading," *Engineering Fracture Mechanics*, vol. 75, no. 18, pp. 5042–5056, 2008.

[7] O. Asi, A. Can, J. Pineault, and M. Belassel, "The effect of high temperature gas carburizing on bending fatigue strength of SAE, 8620 steel," *Materials & Design*, vol. 30, no. 5, pp. 1792–1797, 2009.

[8] M. Liu, A. S. Meyer, D. Fernando, D. A. S. Silva, G. Daniel, and A. Thygesen, "Effect of pectin and hemicellulose removal from hemp fibres on the mechanical properties of unidirectional hemp/epoxy composites," *Composites Part A: Applied Science and Manufacturing*, vol. 90, pp. 724–735, 2016.

[9] A. Bourmaud, J. Beaugrand, D. U. Shah, V. Placet, and C. Baley, "Towards the design of high-performance plant fibre composites," *Progress in Materials Science*, vol. 97, pp. 347–408, 2018.

[10] J. Müssig, S. Amaducci, A. Bourmaud, J. Beaugrand, and D. U. Shah, "Transdisciplinary top-down review of hemp fibre composites: from an advanced product design to crop variety selection," *Composites Part C: Open Access*, vol. 2, Article ID 100010, 2020.

[11] R. Coste, M. Pernes, L. Tetard, M. Molinari, and B. Chabbert, "Effect of the interplay of composition and environmental humidity on the nanomechanical properties of hemp fibers," *ACS Sustainable Chemistry & Engineering*, vol. 8, no. 16, pp. 6381–6390, 2020.

[12] K. Hemalatha, C. James, L. Natrayan, and V. Swamynadh, "Analysis of RCC T-beam and prestressed concrete box girder bridges super structure under different span conditions," *Materials Today: Proceedings*, vol. 37, Part 2, pp. 1507–1516, 2021.

[13] D. B. Munuswamy, Y. Devarajan, S. Ramalingam, S. Subramani, and N. B. Munuswamy, "Critical review on effects of alcohols and nanoadditives on performance and emission in low-temperature combustion engines: advances and perspectives," *Energy & Fuels*, vol. 36, no. 14, pp. 7245–7268, 2022.

[14] V. Balaji, S. Kaliappan, D. M. Madhuvanesan et al., "Combustion analysis of biodiesel-powered propeller engine for least environmental concerns in aviation industry," *Aircraft Engineering and Aerospace Technology*, vol. 94, no. 5, pp. 760–769, 2022.

[15] S. Kaliappan, S. Mohanamurugan, P. K. Nagarajan, and R. Kamal, "Analysis of an innovative connecting rod by using finite element method," *Taga Journal of Graphic Technology*, vol. 14, pp. 1147–1152, 2018.

[16] S. Thomas, S. A. Paul, L. A. Pothan, and B. Deepa, "Natural fibres: structure, properties and applications," in *Cellulose Fibers: Bio- and Nano-Polymer Composites*, pp. 3–42, Springer, Berlin, Heidelberg, 2011.

[17] A. Bourmaud, H. Dhakal, A. Habrant et al., "Exploring the potential of waste leaf sheath date palm fibres for composite reinforcement through a structural and mechanical analysis," *Composites Part A: Applied Science and Manufacturing*, vol. 103, pp. 292–303, 2017.

[18] M.-P. Ho, H. Wang, J.-H. Lee et al., "Critical factors on manufacturing processes of natural fibre composites," *Composites Part B: Engineering*, vol. 43, no. 8, pp. 3549–3562, 2012.

[19] A. Y. M. A. Azim, S. Alimuzzaman, and F. Sarker, "Optimizing the fabric architecture and effect of γ-radiation on the mechanical properties of jute fiber reinforced polyester composites," *ACS Omega*, vol. 7, no. 12, pp. 10127–10136, 2022.

[20] A. S. Kaliappan, S. Mohanamurugan, and P. K. Nagarajan, "Numerical investigation of sinusoidal and trapezoidal piston profiles for an IC engine," *Journal of Applied Fluid Mechanics*, vol. 13, no. 1, pp. 287–298, 2020.

[21] G. Choubey, D. Yuvarajan, W. Huang, A. Shafee, and K. M. Pandey, "Recent research progress on transverse injection technique for scramjet applications—a brief review,"

International Journal of Hydrogen Energy, vol. 45, no. 51, pp. 27806–27827, 2020.

[22] L. Natrayan and A. Merneedi, "Experimental investigation on wear behaviour of bio-waste reinforced fusion fiber composite laminate under various conditions," *Materials Today: Proceedings*, vol. 37, Part 2, pp. 1486–1490, 2021.

[23] S. Kanniyan, V. Andalgopal, and D. Jose, "A review on nanoparticles based colorimetric detection of toxic ion–chromium," *Journal of International Pharmaceutical Research*, vol. 46, no. 5, pp. 453–456, 2019.

[24] H. Kargarzadeh, I. Ahmad, I. Abdullah, A. Dufresne, S. Y. Zainudin, and R. M. Sheltami, "Effects of hydrolysis conditions on the morphology, crystallinity, and thermal stability of cellulose nanocrystals extracted from kenaf bast fibers," *Cellulose*, vol. 19, pp. 855–866, 2012.

[25] P. H. F. Pereira, H. L. Ornaghi Jr., L. V. Coutinho, B. Duchemin, and M. O. H. Cioffi, "Obtaining cellulose nanocrystals from pineapple crown fibers by free-chlorite hydrolysis with sulfuric acid: physical, chemical and structural characterization," *Cellulose*, vol. 27, pp. 5745–5756, 2020.

[26] H. M. Shaikh, A. Anis, A. M. Poulose et al., "Isolation and characterization of alpha and nanocrystalline cellulose from date palm (*Phoenix dactylifera* L.) trunk mesh," *Polymers*, vol. 13, no. 11, Article ID 1893, 2021.

[27] H.-M. Ng, L. T. Sin, T.-T. Tee et al., "Extraction of cellulose nanocrystals from plant sources for application as reinforcing agent in polymers," *Composites Part B: Engineering*, vol. 75, pp. 176–200, 2015.

[28] F. Kallel, F. Bettaieb, R. Khiari, A. García, J. Bras, and S. E. Chaabouni, "Isolation and structural characterization of cellulose nanocrystals extracted from garlic straw residues," *Industrial Crops and Products*, vol. 87, pp. 287–296, 2016.

[29] A. Mandal and D. Chakrabarty, "Isolation of nanocellulose from waste sugarcane bagasse (SCB) and its characterization," *Carbohydrate Polymers*, vol. 86, no. 3, pp. 1291–1299, 2011.

[30] L. Zhou, H. He, C. Jiang, L. Ma, and P. Yu, "Cellulose nanocrystals from cotton stalk for reinforcement of poly(vinyl alcohol) composites," *Cellulose Chemistry and Technology*, vol. 51, no. 1-2, pp. 109–119, 2017.

[31] R. Moriana, F. Vilaplana, and M. Ek, "Cellulose nanocrystals from forest residues as reinforcing agents for composites: a study from macro- to nano-dimensions," *Carbohydrate Polymers*, vol. 139, pp. 139–149, 2016.

[32] M. H. G. Wichmann, J. Sumfleth, F. H. Gojny, M. Quaresimin, B. Fiedler, and K. Schulte, "Glass-fibre-reinforced composites with enhanced mechanical and electrical properties–benefits and limitations of a nanoparticle modified matrix," *Engineering Fracture Mechanics*, vol. 73, no. 16, pp. 2346–2359, 2006.

[33] Y. Tian, H. Zhang, and Z. Zhang, "Influence of nanoparticles on the interfacial properties of fiber-reinforced-epoxy composites," *Composites Part A: Applied Science and Manufacturing*, vol. 98, pp. 1–8, 2017.

[34] B. Wei, S. Song, and H. Cao, "Strengthening of basalt fibers with nano-SiO_2–epoxy composite coating," *Materials & Design*, vol. 32, no. 8-9, pp. 4180–4186, 2011.

[35] I. E. Uflyand and V. I. Irzhak, "Recent advances in the study of structure and properties of fiber composites with an epoxy matrix," *Journal of Polymer Research*, vol. 28, Article ID 440, 2021.

[36] A. Fadavi Boostani, S. Tahamtan, Z. Y. Jiang et al., "Enhanced tensile properties of aluminium matrix composites reinforced with graphene encapsulated SiC nanoparticles," *Composites Part A: Applied Science and Manufacturing*, vol. 68, pp. 155–163, 2015.

[37] V. Andal and B. Gopal, "Preparation of Cu_2O nano-colloid and its application as selective colorimetric sensor for Ag^+ ion," *Sensors and Actuators B: Chemical*, vol. 155, no. 2, pp. 653–658, 2011.

[38] Y. Devarajan, D. B. Munuswamy, B. T. Nalla, G. Choubey, R. Mishra, and S. Vellaiyan, "Experimental analysis of *Sterculia foetida* biodiesel and butanol blends as a renewable and eco-friendly fuel," *Industrial Crops and Products*, vol. 178, Article ID 114612, 2022.

[39] D. Veeman, M. Swapna Sai, P. Sureshkumar et al., "Additive manufacturing of biopolymers for tissue engineering and regenerative medicine: an overview, potential applications, advancements, and trends," *International Journal of Polymer Science*, vol. 2021, Article ID 4907027, 20 pages, 2021.

[40] M. Tamilmagan, D. Easu, V. P. M. Baskarlal, and V. Andal, "Synthesis, characterisation, design and study of magnetorheological property of nano Fe_2O_3," *International Journal of ChemTech Research*, vol. 8, no. 5, pp. 65–69, 2015.

[41] Y. Tang, X. Yang, R. Wang, and M. Li, "Enhancement of the mechanical properties of graphene–copper composites with graphene–nickel hybrids," *Materials Science and Engineering: A*, vol. 599, pp. 247–254, 2014.